

Generalising Tree-Level Sap Flow Across the European Continent

Ralf Loritz¹, Chen Huan Wu¹, Daniel Klotz², Martin Gauch³, Frederik Kratzert³, and Maoya Bassiouni⁴

¹Karlsruhe Institute of Technology

²Johannes Kepler University Linz

³Google Research

⁴University of California, Berkeley

November 20, 2023

Abstract

Sap flow observations provide a basis for estimating transpiration and understanding forest water use dynamics and plant-climate interactions. This study developed a continental modeling approach using Long Short-Term Memory networks (LSTMs) to predict hourly tree-level sap flow across Europe based on the SAPFLUXNET database. We developed models with varying levels of training sets to evaluate performance in unseen conditions. The average Kling-Gupta Efficiency was 0.77 for gauged models trained on 50 % of time series across all forest stands and was 0.52 for ungauged models trained on 50 % of the forest stands. Continental models matched or exceeded performance of specialized and baseline models for all genera and forest stands, demonstrating the potential of LSTMs to generalize hourly sap flow across tree, climate, and forest types. This work highlights hence the potential of deep learning models to generalize sap flow for enhancing tree to continental ecohydrological investigations.

Hosted file

979710_0_art_file_11597767_s47tgg.docx available at <https://authorea.com/users/462788/articles/687776-generalising-tree-level-sap-flow-across-the-european-continent>

1

2 **Generalising Tree–Level Sap Flow Across the European** 3 **Continent**

4 **Ralf Loritz¹, Chen Huan Wu¹, Daniel Klotz², Martin Gauch³, Frederik Kratzert⁴ and**
5 **Maoya Bassiouni⁵**

6 ¹ Institute of Water and River Basin Management, Karlsruhe Institute of Technology (KIT),
7 Karlsruhe, Germany

8 ² Helmholtz Centre for Environmental Research – UFZ, Department Computational of
9 Hydrosystems, Leipzig, Germany

10 ³ Google Research, Zurich, Switzerland

11 ⁴ Google Research, Vienna, Austria

12 ⁵ Department of Environmental Science, Policy and Management, University of California,
13 Berkeley, CA, USA

14

15 Correspondence to: Ralf Loritz (Ralf.Loritz@kit.edu)

16 **Key Points:**

- 17 ● LSTMs demonstrate their ability in predicting hourly sap flow for diverse trees and
18 climates across Europe.
- 19 ● Training on extensive datasets enhances LSTM's ability to simulate sap flow accurately
20 in both seen and unseen environments.
- 21 ● The study underscores the value of large-scale deep learning models and advocates for
22 the expansion of datasets like SAPFLUXNET.
23

24 Abstract.

25 Sap flow observations provide a basis for estimating transpiration and understanding forest water
26 use dynamics and plant-climate interactions. This study developed a continental modeling
27 approach using Long Short-Term Memory networks (LSTMs) to predict hourly tree-level sap
28 flow across Europe based on the SAPFLUXNET database. We developed models with varying
29 levels of training sets to evaluate performance in unseen conditions. The average Kling-Gupta
30 Efficiency was 0.77 for gauged models trained on 50 % of time series across all forest stands and
31 was 0.52 for ungauged models trained on 50 % of the forest stands. Continental models matched
32 or exceeded performance of specialized and baseline models for all genera and forest stands,
33 demonstrating the potential of LSTMs to generalize hourly sap flow across tree, climate, and
34 forest types. This work highlights hence the potential of deep learning models to generalize sap
35 flow for enhancing tree to continental ecohydrological investigations.

36

37 Plain language summary.

38 Transpiration is the dominant flux of water from the land surface to the atmosphere, yet it
39 remains challenging to measure and estimate especially given different climates and tree types.
40 This study shows how large-scale deep learning models can simulate sap flow, the movement of
41 water within trees, with high precision, even in forests and conditions not previously studied. We
42 show that these models excel when they learn from large and diverse datasets. The flexible
43 design of our model training means that every new sap flow measurement can potentially be
44 used to further optimize our networks. Our findings indicate that this approach of continuously
45 updating the model with new information greatly improves its performance to simulate and
46 predict tree-level sap flow. This work thus highlights the potential of deep learning models to
47 generalize sap flow, thereby enhancing ecohydrological investigations from the tree to the
48 continental scale.

49 1 Introduction

50 Accurate quantification of plant transpiration is a critical component in hydrological research,
51 accounting for approximately 65 % of global terrestrial evapotranspiration (e.g. Good et al.,
52 2015). Plants play thereby a pivotal role in controlling the exchange of water between the
53 atmosphere and the land surface. Yet, capturing complex plant water use responses to
54 environmental conditions and estimating transpiration across spatio-temporal scale, remains
55 challenging. Among the limited number of available measurements for plant transpiration, in-situ
56 sap flow sensors are the most widespread technique due to their (relative) low cost and ease of
57 use (Dugas et al., 1993). Sap flow has long been recognized, especially in ecology and plant
58 physiology fields, as a fundamental measurement for deciphering vegetation functionality and
59 transpiration dynamics in both forested (Granier & Loustau, 1994) and agricultural ecosystems
60 (Dugas et al., 1994).

61
62 While the analysis of sap flow has been less prevalent in catchment hydrology, recent studies
63 highlight how sap flow measurements can enhance understanding of intricate relationships
64 among vegetation characteristics, hydrometeorological factors, and catchment properties. For
65 instance, Hassler et al. (2018) conducted an extensive study to determine the relative influence of
66 tree-, stand-, and site-specific characteristics on sap velocity patterns, using data from 61 beech
67 and oak trees across 24 sites in Luxembourg. Their findings suggest that transpiration estimates
68 at the catchment scale could be significantly improved by taking into account not just hydro-
69 meteorological drivers, but also the spatial patterns of the composition of forests in a catchment.
70 Renner et al. (2016) showed that variability in sap flow driven by topography and aspect could
71 be balanced out by the forest stand composition, resulting in equivalent transpiration rates across
72 south and north facing hillslopes. This exemplifies how vegetation dynamics adapt to
73 environmental conditions to effectively use available resources. Hoek van Dijke et al. (2019)
74 used sap flow measurements to explore the link between normalized difference vegetation index
75 (NDVI) and transpiration. They showed that NDVI is not always reliable for modeling
76 transpiration, especially during drought periods, as the correlation between NDVI and sap flow
77 can vary positively or negatively, influenced by seasonal changes, moisture availability, and
78 hydrogeological factors. Integrating sap flow into catchment studies and understanding its spatio-
79 temporal variability is thus key for improving our ability to estimate transpiration at landscape
80 scales

81
82 Sap flow measurement campaigns have typically been designed to examine plant-soil interaction
83 at plot or plant scales (e.g. Jacksich et al., 2020, Seeger et al., 2022). Nevertheless, recent
84 modeling demonstrates avenues for incorporating individual sap flow measurements to advance
85 our understanding of large-scale ecohydrological dynamics, for instance, by validating large
86 scale environmental models and / or by improving catchment wide transpiration estimates (Loritz
87 et al., 2022). Further, the SAPFLUXNET initiative was founded to combine and harmonize
88 numerous, individual small-scale field campaigns in a global open-source sap flow database and
89 hence overcome the spatial and temporal scarcity of sap flow data sets (Poyatos et al., 2021). The
90 SAPFLUXNET database therefore presents unique opportunities to learn generalizable
91 relationships across different plant genera and different climates, critical for estimating sap flow
92 in ungauged regions at the tree level. Such relationships have yet to be encoded into data-driven
93 models to predict sap flow regionally based on tree type, stand characteristics and climate.

94
95 Deep learning offers powerful avenues to find generalizations in large and diverse datasets (e.g.
96 LeCun et al., 2015). For example, Koppa et al. (2022) employed a feed-forward neural network
97 to analyze daily, global datasets from eddy covariance stations, satellites and sap flow
98 measurements from SAPFLUXNET. Their aim was to create an accurate global vegetation stress
99 model that improves simulations of the reduction of evaporation from its theoretical maximum,
100 for instance during periods of water limitations. By integrating the feed-forward neural network

101 into an existing process-based model, they improved the ability of the process-based model to
102 estimate global evaporation rates. Further, Loritz et al. (2022) showed that gated recurrent units
103 (Cho et al., 2014), a form of recurrent neural network that drops old information as it ingests new
104 information, could simulate vegetation dynamics in form of catchment-averaged sap velocities
105 with low residuals even in areas where the model has not been trained. Similar to Koppa et al.
106 2022, Loritz et al. (2022) showed that the deep-learning-based sap velocity simulations can be
107 coupled with a process-based, hydrological model, in this case with the objective to replace the
108 semi-empirical Steward-Jarvis equation, resulting in more accurate transpiration estimates and
109 ultimately better soil moisture simulations particularly during a drought year. In addition, Li et
110 al. (2022), highlighted the ability of recurrent neural networks to estimate the vegetation
111 dynamics of a specific tree species in New Zealand from standard meteorological variables. Both
112 Loritz et al. (2022) and Li et al. (2022) found that particular recurrent neural networks like Long
113 Short-Term Memory (LSTM; Hochreiter and Schmidhuber, 1997) models are suitable
114 architectures to simulate and predict sap flow when they compared different networks. However,
115 both studies trained models on relatively small and local datasets, representing only the dynamics
116 of a forest stand or a small catchment without deciphering different tree species behavior. The
117 extent to which recurrent neural networks can detect consistent relationships between tree-level
118 sap flow and meteorological drivers across different species, measurement methods, climates and
119 forest stands remains an open question.

120

121 This study aims to investigate the potential of LSTMs, a well-suited architecture for simulating
122 environmental time series (e.g. Shen et al., 2017, Kratzert et al., 2018, 2019, Besnard et al.,
123 2019), for modeling tree-level sap flow at an hourly time scale across the European continent.
124 We developed continental tree-level sap flow models leveraging the SAPFLUXNET database to
125 extract generalized relations between sap flow from different tree genera, dynamic atmospheric
126 drivers and forest stand characteristics. We developed different experimental training setups with
127 the aim of evaluating the performance of continental deep learning sap flow models in-sample
128 and out-of-sample against simple baseline models and more specialized, local models. Such a
129 deep learning approach for continental tree-level sap flow modeling offers avenues to overcome
130 limitations of transpiration models when tree-level parameterizations for stomatal conductance
131 are locally unavailable, could be used to assess different forest structures and their implications
132 for regional transpiration rates, and ultimately provide robust sap flow based transpiration
133 estimates across scales.

134 **2 Material and Methods**

135 2.1 The SAPFLUXNET database

136 The SAPFLUXNET database (Poyatos et al., 2021) represents a comprehensive global
137 repository of tree-level sap flow measurements and their ancillary data including tree and forest
138 characteristics and meteorological observations. We used version 0.1.5 of the database

139 encompassing 202 datasets providing information on 2714 individual trees. The sap flow
140 datasets span 174 species (141 angiosperms and 33 gymnosperms), 95 genera, and 45 families
141 and covers the temporal period 1995-2018. The measurement periods for individual trees within
142 the database extends from a minimum of 3 months up to a maximum of 16 years.

143 2.1.1 A European subset of the SAPFLUXNET database

144 We selected a European subset of the SAPFLUXNET dataset, comprising 64 forest stands out of
145 202 stands in the global datasets, encompassing 738 individual trees. We specifically focused on
146 the European subset of SAPFLUXNET due to the high density of measurements and strong
147 overlap of tree genera found within this region. In total, we included six tree genera with > 20
148 individual tree measurements: 282 plants with *Pinus*, 159 plants with *Picea*, 144 plants with
149 *Quercus*, 94 plants with *Fagus*, 30 plants with *Larix*, and 29 plants with *Pseudotsuga*. Selected
150 datasets represented six forest types according to the International Geosphere-Biosphere
151 Programme (IGBP) classification: 34 evergreen needle-leaf forest (ENF), 11 mixed forest (MF),
152 8 deciduous broadleaf forest (DBF), 5 deciduous needle-leaf forest (DNF), 4 evergreen broadleaf
153 forest (EBF), and 2 savannas (SAV). We treated each individual tree seasonal sap flow time
154 series separately resulting in a total of 2279 years of sap flow ($\text{cm}^3 \text{h}^{-1}$) observations, each
155 corresponding to about one vegetation season (April to September, 3-6 months depending if the
156 sensor was installed for a shorter period). The division into individual seasonal time series is
157 important and allows us to include all sensors in our study, even if they cover only a few months
158 at any possible point in time. The winter period (October to March) was excluded as
159 transpiration is low or zero at most stands.

160 2.1.2 Selected model features

161 We considered six dynamic features comprising meteorological variables at an hourly resolution
162 available in the SAPFLUXNET database: air temperature ($^{\circ}\text{C}$), relative humidity (%), vapor
163 pressure deficit (kPa), shortwave incoming radiation (W m^{-2}), precipitation (mm), and wind
164 speed (m s^{-1}). We considered six static features, comprising four forest stand characteristics:
165 mean elevation (m), long-term mean annual temperature ($^{\circ}\text{C}$), long-term mean annual
166 precipitation (mm), and forest type (DBF, DNF, EBF, ENF, MF, SAV), and two individual tree-
167 level characteristics: diameter at breast height (DBH; cm) and tree genera (*Fagus*, *Larix*, *Picea*,
168 *Pinus*, *Pseudotsuga*, and *Quercus*). We implemented one-hot-encoding for each of the 6 genera
169 and 6 forest types in the dataset. We note that we included the DBH as a scaling variable in the
170 model features to adequately estimate tree-level sap flow instead of standardizing and upscaling
171 the sap flow measurements into transpiration rates per unit area. As such, one can apply the
172 resulting models in unseen locations, potentially test novel stand structure scenarios and have the
173 flexibility to estimate forest-level transpiration given different tree genera, sizes, and density.

174 2.2 Deep learning model - Long Short-Term Memory

175 LSTMs are recurrent neural networks that are specifically engineered to circumvent the
176 vanishing and exploding gradient problem encountered in regular recurrent neural networks
177 (Hochreiter and Schmidhuber, 1997; Hochreiter 1998). This is achieved through the introduction
178 of a cell state, which provides the network with the capability to learn long-term dependencies
179 that are typically important in environmental, sequential data. The memory cell works in
180 conjunction with so-called "gates", mechanisms that evolve the memory and output over time,
181 while allowing the error to propagate consistently through the network, thereby facilitating the
182 learning process. LSTMs have showcased their efficiency and aptitude in hydrological modeling
183 and have emerged as one of the top-performing models for simulating various state-dependant
184 ecohydrological phenomena, such as streamflow, soil moisture and ecosystem water and carbon
185 fluxes (e.g. Kratzert et al., 2018; 2019, Besnard et al., 2019; Bartolomeis et al., 2023).

186 2.2.1 LSTM hyperparameters

187 We explored ranges of LSTM hyperparameter settings based on previous hydrological studies
188 (Mai et al., 2022) and saw that the LSTM performance was relatively stable with a wide range of
189 hyperparameters. Thus, for the sake of simplicity, we only show the results of a single set of
190 parameters here. We chose the settings from Mai et al. 2022, with modifications made to (1) a
191 reduced sequence length (which represents the number of time steps the network looks back to
192 process and learn from sequential inputs) and (2) a reduced number of epochs. Both changes
193 only minimally influenced the model performance while greatly decreasing training times of the
194 LSTMs. The hyperparameter setting used for all model variants are: number of hidden layers =
195 1; hidden layer neurons = 256; learning rate = 0.0005; dropout rate = 0.4; batch size = 64;
196 sequence length = 24 hours; epoch 20; iterative optimization algorithm = ADAM.

197 2.2.2 Model setups and evaluation

198 We developed several experimental setups that differ in the amounts of data that were used to
199 train the models with the goal of testing the model performance in different conditions. Our
200 objective is to compare simple baseline, specialized and continental model setups 1) to assess the
201 value of training deep learning models on larger and more diverse datasets instead of building
202 models for each site or genera and 2) quantify model performance in predicting sap flow for
203 unseen periods and for unseen locations.

204
205 For all model setups, the data were divided such that a single vegetation growing season of tree-
206 level sap flow data is treated as an individual time series and entirely part of either the training,
207 validation or test data (in total 2279 individual time series). We split the 2279 individual time
208 series ten times into 1140 years (50%) for training, 912 years (40%) for testing and set aside the
209 remaining 227 years (10 %) for validation. This so-called Monte Carlo Cross Validation scheme
210 allows us to assess the robustness of our models with respect to the information content of the

211 training data by training LSTMs on ten different random subsamples that are drawn without
212 repetitions (Maier et al., 2023). We assessed each model's performance using the Kling-Gupta
213 efficiency (KGE) and its three components: Pearson correlation (r), bias ratio (α), and variability
214 ratio (β), the Nash-Sutcliff efficiency (NSE), and the mean absolute error (MAE). For definitions
215 of these performance metrics please see Gupta et al. (2009). All numeric input features were
216 standardized by subtracting the mean and by dividing them by the standard deviation of the
217 training data.

218
219 We developed two types of specialized models that have been trained on smaller subsets of the
220 data described in section 2.1.1: For the single forest stand models, we trained LSTMs on a single
221 forest stand (location) at a time and across several tree genera; if present at the forest stand. For
222 the single tree genera models, we trained LSTMs on a single genera at a time (e.g. Fagus, Pinus)
223 and across several forest stands where the genera is present. Further we trained gauged-
224 continental models across all 64 forest stands. With the gauged-continental models, we assess the
225 ability of the LSTMs to generalize in new time periods but in seen forest stands. Finally, we
226 compare gauged-continental models to gauged-baseline models, representing the monthly
227 averaged hourly diurnal cycle of sap flow for each stand and for each genera across the European
228 continent. These baseline models are built ten times on the same randomly selected training data
229 as the gauged-continental models.

230
231 We developed ungauged-continental models to fully examine the LSTM networks' ability to
232 generalize at unseen forest stands and trees. We divided the data into random subsets of 50 %
233 training (33 stands) and 50 % testing (31 stands). We stratified the splits to maintain the fractions
234 of forest type (IGBP) within each split (Kang et al., 2023). For the forest type evergreen broad-
235 leaved forest (EBF), which had three stands, two were used for training and one for testing. The
236 total number of stands for training was 33 versus 31 stands for testing. We compare ungauged-
237 continental models to ungauged-baseline models, representing the monthly averaged hourly
238 diurnal cycle of sap flow for each genera across the european continent. These ungauged-
239 baseline models are built ten times on the same training data as the ungauged-continental
240 models.

241 **3 Results**

242 3.1 Performance of gauged-continental models

243 The gauged-continental models, representing the upper bound in performance, were capable of
244 simulating sap flow with an average KGE of 0.77 ± 0.04 (Figure. 1) in comparison to the
245 gauged-baseline models of 0.64 ± 0.05 . The comparison is, however, in favor of the gauged-
246 baseline models as not all stands have several trees with the same genera and as we use a random
247 subsampling to generate our training data. The latter entails that the genera-specific monthly
248 averaging works only at sites with several sensors or long observation time series where we

249 typically also observe higher performances of the gauged-continental models. The performance
250 differences between the ten random training splits were small (± 0.04 KGE). This indicates that
251 the randomly selected training data each hold a similar amount of information about the
252 relationship between input features and sap flow and that the model is capable of generalizing.
253 Looking closely at model performance across tree genera, there is a consistent pattern of high
254 KGE values for *Quercus*, *Fagus*, and *Pseudotsuga* trees. Notably, even *Pseudotsuga*, the tree
255 genera with one of the smallest dataset (80 years), achieves a KGE of 0.76 ± 0.07 in contrast to
256 a KGE of 0.34 ± 0.07 for the gauged-baseline model. On the other hand, sap flow simulations of
257 the *Picea* trees showed weaker performances with KGEs of 0.55 ± 0.06 , despite being frequently
258 found in the data (gauged-baseline models = 0.28 ± 0.03). The amount of data for a tree genera
259 does not directly correlate with the model performance.

260

261 Figure. 2 illustrates three sequences of hourly sap flow simulations and observations of a
262 *Quercus* tree, a *Pseudotsuga* tree and a *Picea* tree for five consecutive days. While there is some
263 uncertainty, most models of the ensemble agree on the diurnal sap flow pattern, which is
264 underpinned by the fact that Pearson correlations between different members of the model
265 ensemble are all higher than 0.8. In agreement with the overall findings, the gauged-continental
266 models capture the sap flow dynamics from the shown *Quercus* tree well (Pearson correlation =
267 0.9) and also match the absolute values ($\beta = 1.03$). The model performance for the shown *Picea*
268 tree was lower and matches the dynamics to a certain extent (Pearson correlation = 0.77) but
269 misses the absolute values. For the *Pseudotsuga*, the patterns and absolute values are well
270 matched and even the drop of sap flow during midday for two days is matched reasonably well
271 by the gauged-continental model. Model uncertainty across random subsampling is low for both
272 the *Quercus* and *Pseudotsuga* tree compared to the *Picea* tree.

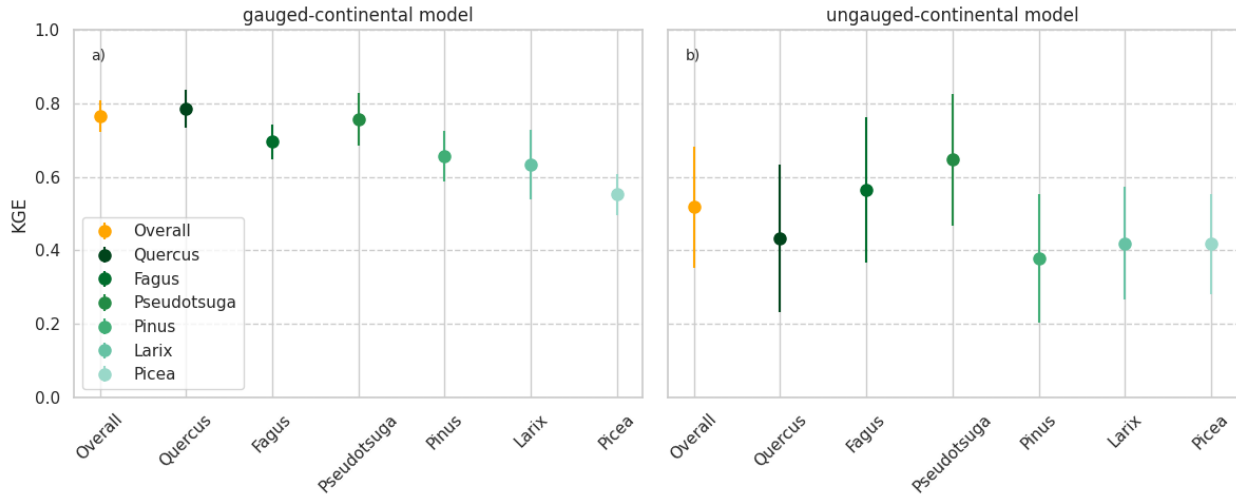
273 3.2 Performance of specialized models

274 Overall, models trained on a single genera did not outperform the gauged-continental models. At
275 best they achieved an equivalent performance to the gauged-continental models. However, single
276 genera models were found to be more sensitive to the amount of data, particularly if trained only
277 on a few sites, and can exhibit large performance differences, even leading to negative KGEs for
278 some tree genera. In contrast, the gauged-continental models remain relatively stable and less
279 affected if the data representing a genera is reduced or if the number of stands is varied. Here, no
280 simulation, not even removing a tree genera completely, resulted in a negative KGE. This opens
281 the avenue to extend the training dataset by new tree types even if they have only been measured
282 at a few locations for a short period.

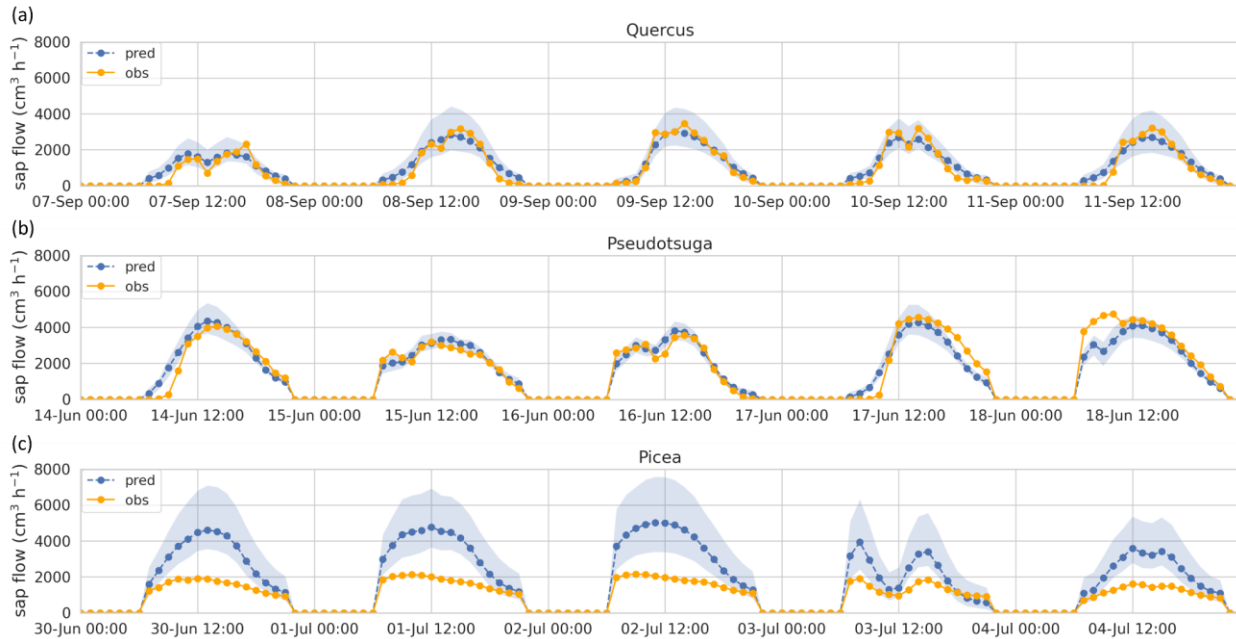
283

284 We also compared the outcomes of the single-stand and gauged-continental models, focusing on
285 the specific tree genera measured at each site as not all tree types are present in each forest stand.
286 At certain forest stands, for example in some locations in central Europe, the performance of the
287 single stand models closely mirrors the gauged-continental model for the dominant genera at

288 these sites (*Fagus*). On the other hand, in some locations in South France, performance was
 289 lower than the gauged-continental model for the dominant genera (*Quercus* trees) with KGEs
 290 around 0.5 or 0.6 versus KGEs of 0.79. At no forest stand did the single-stand models
 291 outperform the gauged-continental model.



292 **Figure 1:** Performance and standard deviation (\pm) of the ten a) gauged-continental models and b) the ten ungauged-continental models measured by the KGE for all testing data (overall; orange) and for each of the six tree genera (genera name; green).
 293
 294
 295



296 **Figure 2:** Observed and simulated hourly sap flow using the gauged-continental model for five consecutive days in the testing data for a) a
 297 *Quercus* tree in the year 2011 (France), b) a *Pseudotsuga* tree in the year 2012 (Germany) and c) for a *Pinus* tree in the year 2001 (Sweden). Blue
 298 bands visualize the uncertainty of the gauged-continental model given the five random training subsampling.
 299

300 3.3 Performance of ungauged-continental models

301 As expected, the performance of the ungauged-continental model is on average lower than that
 302 of the gauged-continental model yet proved reasonable with an average KGE of 0.52 ± 0.16 in
 303 comparison to a KGE of -0.11 ± 0.15 of the ungauged-baseline model. The difference for the

304 genera-specific performance is also in this range with the highest difference of 0.79 (KGE) for
305 *Quercus* trees (ungauged-baseline models = 0.43 and ungauged-continental models = -0.36).
306 Model performance of the ungauged-continental models increased rather quickly if, for instance,
307 70 % instead of 50% of the data was used for training (KGE \approx 0.65). Diving into the individual
308 models, we found that the performance was particularly affected by the frequency of forest types,
309 despite stratifying random subsampling of the training data by IGBP. In other words, forest types
310 with lower frequencies had a larger effect on the overall test scores than the amount of samples
311 of a tree genera. The observed performance variance of the ungauged-continental models
312 (standard deviation of 0.16) highlights the variability of the information content in the training
313 data. Again this value reduces rather quickly if the models are trained on more data.

314 **4 Discussion**

315 4.1 Gauged-continental models provide robust sap flow estimates across the European 316 continent compared to specialized and baseline models

317 Gathering sap flow data can result in strong variations even at the same tree, making it
318 challenging to achieve consistent and accurate readings (Steppe et al., 2010). For instance, sap
319 flow measurements taken just a few meters apart in trees of similar genera, size, and height can
320 show significant differences (Vandegehuchte and Steppe, 2013). Particularly absolute values
321 vary, while the overall dynamics, akin to what is frequently found with respect to in-situ soil
322 moisture observations, are typically well-matched if similar sensors are installed in different
323 trees located in the same forest stand (e.g. Zehe et al., 2005; Loritz et al., 2017; Hassler et al.,
324 2018). Differences in absolute values might thereby arise from various small-scale structural
325 characteristics, such as properties of the sap wood or heterogeneous flow paths inside the stem.
326 These factors are typically unknown and not provided to our models as input. The model has,
327 therefore, no way to learn such small-scale differences that might explain why at two similar
328 trees in close proximity different absolute sap flows have been measured. This might be one
329 reason why all models in this study generally learn to represent the dynamics of sap flow well,
330 but can exhibit a high bias for certain trees. Nevertheless, given that SAPFLUXNET uses various
331 sensors and measurement techniques across the globe (see the discussion of the SAPFLUXNET
332 publication during the review process in *Earth System Science Data*; Poyatos et al., 2021) it is
333 striking that LSTMs can generalize tree-level sap flow across diverse climate zones and genera
334 with a performance akin to the local models described by Li et al. (2022), Loritz et al. (2022) and
335 the specialized models trained in this study (e.g. in terms of sensor type, installing method, tree
336 type, climate zone). Our findings reinforce thereby previous research suggesting that deep
337 learning models, trained on large and diverse datasets, often outperform those trained on more
338 localized, less diverse data (e.g. Kratzert et al., 2019, Sunwook and Steinschneider, 2022). While
339 many single genera or single stand models (specialized models) in our study performed
340 comparably to the gauged-continental models, there were notable instances where the latter was

341 superior. The gauged-continental models displayed reduced variance during the random
342 subsampling of the training data and are able to simulate a tree genera even if it was entirely
343 omitted with a KGE ranging from 0.2 to 0.4 depending on the tree genera. This result indicates
344 that forest type (IGBP) provides more valuable insights for the models than information about
345 which specific tree genera it should simulate. The reason being, variations within some of the
346 forest types are less even among different tree genera, than those across forest types.

347 4.2 Ungauged-continental LSTMs provide reasonable sap flow estimates at ungauged
348 forest stands, and new data have the potential to further enhance this capability

349 We quantified LSTMs performance for predicting hourly sap flow at forest stands that were
350 unseen during training. The results show that the overall ungauged-continental model's
351 performance, although lower than that of the gauged-continental model, was still reasonable with
352 an average KGE of around 0.52. We found that the best-performing forest stands were often in
353 the most frequent forest types (e.g. ENF). While the model was capable of predicting sap flow
354 also in boreal and mediterranean forests, where measurements are more scarce, these predictions
355 became less reliable the further they deviated from the training data showing clear limitations of
356 the ungauged-continental model and the chosen training data set. The random subsampling of the
357 training data and experiments with increasing the training data highlight that each new set of sap
358 flow data can make the LSTM more robust, particularly in vegetation types that are less
359 frequently monitored. Given that there are many tax funded large sap flow datasets available in
360 Europe (and likely in other parts of the world) that are yet not openly available and not included
361 in SAPFLUXNET, we argue that our study hints towards the currently unused potential that lies
362 ahead when these data sets are shared in a consistent manner or if new measurement campaigns
363 would be designed specifically to close the spatial and ecological gaps in the SAPFLUXNET
364 dataset.

365
366 The ungauged-continental models can make reasonable hourly predictions of sap flow in unseen
367 forest stands for a majority of the European continent. This entails that with prescribed forest
368 type and weather data (e.g. from climate models), it is possible to create hourly sap flow maps
369 for Europe with one, continental deep learning model. Surely these dynamic maps have clear
370 limitations but there are limited options to gather hourly information about plant water use at the
371 tree level at ungauged sites. Furthermore, as we simulate tree-level sap flow based on different
372 forest stand characteristics (DBH, genera) this model could be used to assess different forest
373 structures and their implications for regional transpiration rates and how they potentially change
374 under different forest management strategies. Such dynamic sap flow maps could also be used to
375 evaluate or replace transpiration models that are frequently found in land surface or hydrological
376 models as shown in Loritz et al. (2022). Our study hence demonstrates an avenue towards
377 developing ensembles of continental sap flow models to predict sap flow and evaluate vegetation
378 dynamics around the globe.

379 **5. Conclusion**

380 This study evaluated the current potential and limits of deep learning to generalize tree-level sap
381 flow dynamics across the European continent. Key technical criteria for developing robust
382 LSTMs include the random subsampling strategy based on the vegetation seasons and the
383 requirement to train the networks on large and diverse data. If trained properly we demonstrate
384 that LSTMs can achieve a reasonable level of performance in predicting hourly sap flow for
385 different tree genera, climate zones and forest types. Training deep learning models on large and
386 diverse datasets and on several tree genera at the same time proved beneficial compared to
387 specialized models and supported that LSTMs are capable generalizing vegetation dynamics
388 beyond the individual tree-level sap flow measurement. This research paves the way for
389 producing hourly tree-level sap flow maps across Europe, harnessing the combination of forest
390 characteristics and dynamic meteorological drivers. Our study hints that as more sap flow
391 datasets become openly available, the accuracy and coverage of such models are expected to
392 improve significantly particularly for forest types that are less frequently found in the
393 SAPFLUXNET dataset. This holds the promise of increasing our ability to simulate the
394 vegetation water use dynamics that are encoded in sap flow and could serve as a valuable
395 benchmark for different land surface and hydrological models.

396 **Acknowledgments**

397 This research contributes to the ViTamins (Invigorating Hydrological Science and Teaching:
398 merging key Legacies with new Concepts and Paradigms) Project funded by the Volkswagen
399 Foundation.

400

401 **Open Research**

402 SAPFLUXNET is openly available at <https://zenodo.org/records/3971689>. All python codes to
403 run the models are openly available at: [10.5281/zenodo.10118262](https://zenodo.org/records/10118262).

404

405 **References**

406 de Bartolomeis, P., Meterez, A., Shu, Z., & Stocker, B. D. (n.d.). An effective machine learning
407 approach for predicting ecosystem CO₂ assimilation across space and time. doi:
408 [10.5194/egusphere-2023-1826](https://doi.org/10.5194/egusphere-2023-1826)

409

410 Besnard, S., Carvalhais, N., Altaf Arain, M., Black, A., Brede, B., Buchmann, N., Chen, J.,
411 Clevers, J. G. P. W., Dutrieux, L. P., Gans, F., Herold, M., Jung, M., Kosugi, Y., Knohl, A.,
412 Law, B. E., Paul-Limoges, E., Lohila, A., Merbold, L., Roupsard, O., ... Reichstein, M. (2019).
413 Memory effects of climate and vegetation affecting net ecosystem CO₂ fluxes in global forests.
414 *PLoS ONE*, 14(2). doi: [10.1371/journal.pone.0211510](https://doi.org/10.1371/journal.pone.0211510)

415

- 416 Cho, K., van Merriënboer, B., Gulcehre, C., Bahdanau, D., Bougares, F., Schwenk, H., &
417 Bengio, Y. (2014). Learning Phrase Representations using RNN Encoder-Decoder for Statistical
418 Machine Translation. <http://arxiv.org/abs/1406.1078>
419
- 420 Dugas, W. A., Wallace, J. S., Allen, S. J., & Roberts, J. M. (1993). Heat balance, porometer, and
421 deuterium estimates of transpiration from potted trees. *Agricultural and Forest Meteorology*,
422 *64*(1–2), 47–62. doi: 10.1016/0168-1923(93)90093-W
423
- 424 Dugas, W. A., Heuer, M. L., Hunsaker, D., Kimball, B. A., Lewin, K. F., Nagy, J., & Johnson,
425 M. (1994). Sap flow measurements of transpiration from cotton grown under ambient and
426 enriched CO₂ concentrations. *Agricultural and Forest Meteorology*, *70*(1–4), 231–245. doi:
427 10.1016/0168-1923(94)90060-4
428
- 429 Good, S. P., Noone, D., & Bowen, G. (2015). Hydrologic connectivity constrains partitioning of
430 global terrestrial water fluxes. *Science*, *349*(6244), 175–177. doi: 10.1126/science.aaa5931
431
- 432 Granier, A., & Loustau, D. (1994). Measuring and modelling the transpiration of a maritime pine
433 canopy from sap-flow data. *Agricultural and Forest Meteorology*, *71*(1–2), 61–81. doi:
434 10.1016/0168-1923(94)90100-7
435
- 436 Gupta, H. v., Kling, H., Yilmaz, K. K., & Martinez, G. F. (2009). Decomposition of the mean
437 squared error and NSE performance criteria: Implications for improving hydrological modelling.
438 *Journal of Hydrology*, *377*(1–2), 80–91. doi: [10.1016/j.jhydrol.2009.08.003](https://doi.org/10.1016/j.jhydrol.2009.08.003)
439
- 440 Hassler, S. K., Weiler, M., & Blume, T. (2018). Tree-, stand- and site-specific controls on
441 landscape-scale patterns of transpiration. *Hydrology and Earth System Sciences*, *22*(1), 13–30.
442 doi: 10.5194/hess-22-13-2018
443
- 444 Hochreiter, S., & Schmidhuber, J. (1997). Long Short-Term Memory. *Neural Computation*, *9*(8),
445 1735–1780. doi: [10.1162/neco.1997.9.8.1735](https://doi.org/10.1162/neco.1997.9.8.1735)
446
- 447 Maier, H. R., Zheng, F., Gupta, H., Chen, J., Mai, J., Savic, D., Loritz, R., Wu, W., Guo, D.,
448 Bennett, A., Jakeman, A., Razavi, S., & Zhao, J. (2023). On how data are partitioned in model
449 development and evaluation: Confronting the elephant in the room to enhance model
450 generalization. *Environmental Modelling & Software*, *167*, 105779. doi:
451 [10.1016/j.envsoft.2023.105779](https://doi.org/10.1016/j.envsoft.2023.105779)
452
- 453 Hoek van Dijke, A. J., Mallick, K., Teuling, A. J., Schlerf, M., Machwitz, M., Hassler, S. K.,
454 Blume, T., & Herold, M. (2019). Does the Normalized Difference Vegetation Index explain
455 spatial and temporal variability in sap velocity in temperate forest ecosystems? *Hydrology and*
456 *Earth System Sciences*, *23*(4), 2077–2091. doi: 10.5194/hess-23-2077-2019
457
- 458 Jackisch, C., Knoblauch, S., Blume, T., Zehe, E., & Hassler, S. K. (2020). Estimates of tree root
459 water uptake from soil moisture profile dynamics. *Biogeosciences*, *17*(22), 5787–5808. doi:
460 [10.5194/bg-17-5787-2020](https://doi.org/10.5194/bg-17-5787-2020)
461

- 462 Kang, Y., Gaber, M., Bassiouni, M., Lu, X., and Keenan, T.: CEDAR-GPP: spatiotemporally
463 upscaled estimates of gross primary productivity incorporating CO₂ fertilization, *Earth Syst. Sci.*
464 *Data Discuss.* [preprint], doi: 10.5194/essd-2023-337, in review, 2023.
- 465
466 Kling, H., & Gupta, H. (2009). On the development of regionalization relationships for lumped
467 watershed models: The impact of ignoring sub-basin scale variability. *Journal of Hydrology*,
468 373(3–4), 337–351. doi: 10.1016/j.jhydrol.2009.04.031
- 469
470 Kratzert, F., Klotz, D., Brenner, C., Schulz, K., & Herrnegger, M. (2018). Rainfall–runoff
471 modelling using Long Short-Term Memory (LSTM) networks. *Hydrology and Earth System*
472 *Sciences*, 22(11), 6005–6022. doi: 10.5194/hess-22-6005-2018
- 473 Kratzert, F., Klotz, D., Shalev, G., Klambauer, G., Hochreiter, S., & Nearing, G. (2019).
474 Towards learning universal, regional, and local hydrological behaviors via machine learning
475 applied to large-sample datasets. *Hydrology and Earth System Sciences*. doi: [10.5194/hess-23-](https://doi.org/10.5194/hess-23-5089-2019)
476 [5089-2019](https://doi.org/10.5194/hess-23-5089-2019)
- 477
478 Koppa, A., Rains, D., Hulsman, P., Poyatos, R., & Miralles, D. G. (2022). A deep learning-based
479 hybrid model of global terrestrial evaporation. *Nature Communications*, 13(1), 1912. doi:
480 [10.1038/s41467-022-29543-7](https://doi.org/10.1038/s41467-022-29543-7)
- 481
482 Lecun, Y., Bengio, Y., & Hinton, G. (2015). Deep learning. In *Nature* (Vol. 521, Issue 7553, pp.
483 436–444). Nature Publishing Group. doi: [10.1038/nature14539](https://doi.org/10.1038/nature14539)
- 484
485 Li, Y., Ye, J., Xu, D., Zhou, G., & Feng, H. (2022). Prediction of sap flow with historical
486 environmental factors based on deep learning technology. *Computers and Electronics in*
487 *Agriculture*, 202. doi: 10.1016/j.compag.2022.107400
- 488
489 Loritz, R., Bassiouni, M., Hildebrandt, A., Hassler, S. K., & Zehe, E. (2022). Leveraging sap
490 flow data in a catchment-scale hybrid model to improve soil moisture and transpiration
491 estimates. *Hydrology and Earth System Sciences*, 26(18), 4757–4771. doi: [10.5194/hess-26-](https://doi.org/10.5194/hess-26-4757-2022)
492 [4757-2022](https://doi.org/10.5194/hess-26-4757-2022)
- 493
494 Mai, J., Shen, H., Tolson, B. A., Gaborit, É., Arsenault, R., Craig, J. R., Fortin, V., Fry, L. M.,
495 Gauch, M., Klotz, D., Kratzert, F., O'Brien, N., Princz, D. G., Rasiya Koya, S., Roy, T.,
496 Seglenieks, F., Shrestha, N. K., Temgoua, A. G. T., Vionnet, V., & Waddell, J. W. (2022). The
497 Great Lakes Runoff Intercomparison Project Phase 4: the Great Lakes (GRIP-GL). *Hydrology*
498 *and Earth System Sciences*, 26(13), 3537–3572. doi: 10.5194/hess-26-3537-2022
- 499
500 Poyatos, R., Granda, V., Flo, V., Adams, M. A., Adorján, B., Agudé, D., Aidar, M. P. M.,
501 Allen, S., Alvarado-Barrientos, M. S., Anderson-Teixeira, K. J., Aparecido, L. M., Altaf Arain,
502 M., Aranda, I., Asbjornsen, H., Baxter, R., Beamesderfer, E., Berry, Z. C., Berveiller, D.,
503 Blakely, B., ... Martínez-Vilalta, J. (2021). Global transpiration data from sap flow
504 measurements: The SAPFLUXNET database. In *Earth System Science Data* (Vol. 13, Issue 6).
505 doi: [10.5194/essd-13-2607-2021](https://doi.org/10.5194/essd-13-2607-2021)
- 506

- 507 Renner, M., Hassler, S. K., Blume, T., Weiler, M., Hildebrandt, A., Guderle, M., Schymanski, S.
508 J., & Kleidon, A. (2016). Dominant controls of transpiration along a hillslope transect inferred
509 from ecohydrological measurements and thermodynamic limits. *Hydrology and Earth System*
510 *Sciences*, 20(5), 2063–2083. doi: [10.5194/hess-20-2063-2016](https://doi.org/10.5194/hess-20-2063-2016)
- 511
512 Seeger, S., & Weiler, M. (2021). Temporal dynamics of tree xylem water isotopes: In situ
513 monitoring and modeling. *Biogeosciences*, 18(15), 4603–4627. doi: [10.5194/bg-18-4603-2021](https://doi.org/10.5194/bg-18-4603-2021)
- 514
515 Steppe, K., de Pauw, D. J. W., Doody, T. M., & Teskey, R. O. (2010). A comparison of sap flux
516 density using thermal dissipation, heat pulse velocity and heat field deformation methods.
517 *Agricultural and Forest Meteorology*, 150(7–8), 1046–1056. doi:
518 10.1016/j.agrformet.2010.04.004
- 519
520 Wi, S., & Steinschneider, S. (2022). Assessing the Physical Realism of Deep Learning
521 Hydrologic Model Projections Under Climate Change. *Water Resources Research*, 58(9). doi:
522 10.1029/2022WR032123
- 523
524 Vandegehuchte, M.W. and Steppe, K. 2013. Corrigendum to: Sap-flux density measurement
525 methods: working principles and applicability. *Functional Plant Biology* 40(10), 1088-1088. doi:
526 10.1071/FP12233_CO
- 527
528 Zehe, E., Graeff, T., Morgner, M., Bauer, A., & Bronstert, A. (2010). Plot and field scale soil
529 moisture dynamics and subsurface wetness control on runoff generation in a headwater in the
530 Ore Mountains. *Hydrology and Earth System Sciences*, 14(6), 873–889. doi: 10.5194/hess-14-
531 873-2010